DOI:
10.1109/MRA.2016.2580478

Robotic Ultrasound: View Planning, Tracking, and Automatic Acquisition of Trans-esophageal Echocardiography

Automatic ultrasound acquisitions using medical robots would greatly increase the general usability of medical ultrasound with the abilities of remote control and built-in intelligence. This requires novel methods to provide an overall workflow linking robotic systems with ultrasound acquisitions. Based on a newly developed robot for Trans-esophageal echocardiography (TEE), we propose a view planning platform, an auto-adaption method for patient-specific data, and an image-based probe tracking method. With all these ingredients, a phantom experiment was performed with both open-loop and closed-loop positioning methods aiming at proving the concept of the automatic ultrasound acquisition. The results demonstrate the feasibility of the whole workflow and indicate high accuracy of acquisition in terms of keeping desired anatomies in the field of view.

Automatic Ultrasound Acquisition

Medical ultrasound is an important imaging modality which can provide real-time evaluation of patients. Compared with many other modalities, an ultrasound scanner is portable, substantially lower in cost, and it does not use harmful ionizing radiation. In many intraoperative cases, ultrasound is especially useful, as it can guide the surgery by providing real-time images of otherwise hidden devices and anatomy. In this study, we are particularly interested in trans-esophageal echocardiography (TEE). This can be used for diagnosing heart disease and guiding cardiac surgical procedures using either 2-D or 3-D ultrasound imaging [1, 2]. However, operation of this technique, similar to acquisitions of extracorporeal ultrasound, still requires manual control, which greatly depends on the on-site operator. The on-site operation of ultrasound systems usually exposes operators to an undesirable working environment which could potentially cause occupational injuries [3]. Particularly for TEE in minimally-invasive interventional procedures, the operator may be exposed to ionizing radiation from X-ray C-arms and have to wear uncomfortable and bulky shielding [4]. These problems may be addressed by remotely operated ultrasound systems employing robotic techniques. Our previous design of the first TEE robot has demonstrated the capability of remote control [5].

However, remote controlled ultrasound systems are not adequate to solve the problem of general usability of medical ultrasound as they still require a manual control approach which is tedious, time consuming, and most of all totally operator-dependent. In both developed and developing countries, because of the requirement for highly specialized skills during ultrasound acquisition, small clinics in remote locations are unlikely to have ultrasound experts available most of the time [6]. It has been suggested that the lack of ultrasound training is one of the biggest barriers to reliable image acquisitions [7, 8]. The problem of skills and trainings is made worse by the views of the heart being relatively complicated to understand. Therefore, intelligence towards automatic or semi-automatic ultrasound acquisitions has to be built into these robotic medical ultrasound systems in order to achieve a breakthrough in the utilization of ultrasound with robots.

There are a few existing works on robotic assisted acquisitions for extracorporeal ultrasound [9]. Several works explore visual servoing techniques for tracking particular features, e.g. tracking the carotid artery using an extracorporeal ultrasound robot [10]. Further works have been extended by other researchers to automatic scanning of the carotid artery using motion compensation [11]. The idea of a vision-based self-guided system is also employed in other types of medical robots, such as an eye-in-hand endoscopic robotic system used for physiology motion rejection in natural orifice transluminal endoscopic surgery where the robot is used for tracking an area of interest despite breathing motion [12]. In other robotic domains, visual servoing is also one of the most important techniques widely used for manufacturing, object picking, teleoperation, missile tracking, etc. A comprehensive review of those works is given in [13]. However, using visual servoing techniques based on feature extraction for cardiac ultrasound acquisitions is challenging due to the complexity of the heart structure. Since global information of the heart from MR or CT images always exist in many cardiac surgical procedures, we believe that using pre-planned motion and multi-modality registration is the preferred approach to deal with vision and motion. To our knowledge, no such system has been proposed for cardiac echocardiography, and we present a unique study providing a complete solution for automatic imaging of the heart.

In this study, we aim at providing a view planning solution for trans-esophageal ultrasound views in patient-specific data during cardiac procedures based on a pre-procedure CT or MRI scan. We also develop a method for automatic acquisition of these planned views using our robotic system. This method, though primarily designed for TEE, has the potential to be adapted for other intraoperative ultrasound, such as trans-rectal or intra-cardiac imaging. Other aspects of the proposed TEE robot, including safety and force sensing, have been briefly discussed in our previous work [5]. Since the current paper focuses on automation and tracking, the topics of safety and force sensing are not included here.

Robotic Trans-esophageal Ultrasound System

We have previously developed an add-on robotic trans-esophageal ultrasound system (Fig. 1. a) to operate a commercial TEE probe (X7-2t, Philips Healthcare, The Netherlands), allowing operators to precisely adjust the probe's position remotely. The slave system (the robot) is driven wirelessly via Bluetooth communication and has several mechanisms for holding and manipulating the original probe. Our previous work [5] on evaluating the precision of the robotic system in free space demonstrated a high repeatability of the probe positioning with a mean error of 0.6 mm and 0.3 deg for the translation axis; 1.3 mm and 0.9 deg for axial rotation; and 0.6 mm and 0.8 deg for bi-directional bending. Since each individual degree of freedom is driven by a different motor, multiple axes of the robot can be driven simultaneously in any combination. We have since developed a dummy probe, serving as the master control device, for intuitive remote operation of the robot (Fig. 1. b). This dummy probe has a similar shape to the original TEE probe handle and has built-in sensors to interpret users' inputs. A pair of buttons on the dummy probe is used for driving the linear belt mechanism of the robot for translating the original probe. A rotating handle, which can rotate about the long axis of the dummy probe, is used for driving the gear train mechanism of the robot for rotation of the original probe. A dual-shaft driving knob pair is used for rotating similar knobs on the original probe handle, via the belt mechanism, for bi-directional bending of the probe head.

Planning Platform for Standard Ultrasound Views

We have developed a view-planning platform with a user-friendly interface using Unity (Unity Technologies, USA). This platform allows users to plan and define standard view planes of trans-esophageal ultrasound imaging. A reference heart 3-D image, from an MR image, is automatically segmented including the cardiac chambers and great vessels using shape-constrained deformable models [14]. The corresponding esophagus centre line model is extracted by manual tracing from the same MR image. Both models are loaded into the view planning platform and visualized intuitively.

In this view planning platform, movements of TEE probe are modelled using the forward kinematics, including the translation, rotation, and bi-directional bending of a virtual probe head. Additionally, electronic steering of the ultrasound beam is modelled by rotating the 2-D ultrasound plane. Details of the modelling procedure have been presented in [5]. Desirable views are found by manual interaction with the view-planning software. In the virtual setup, the five robotic parameters are adjusted via sliders in the software, and the resulting view plane is interactively updated to show the imaged 2-D slice. In this way, suitable long and short axis views of the heart are found and the corresponding robotic parameters recorded. Therefore, the platform can be used to define a 2-D ultrasound view directly or a 3-D ultrasound view based on slice views. An example of a 2-D mid-esophageal four-chamber view is shown in Fig. 2 with an explanation of functional components of the view planning platform.

Auto-adaption to Patient-Specific Data

Variations of the heart and esophagus between patients could result in incorrect positioning of desired standard views if the same probe robotic parameters from the reference heart-esophagus model are used for every patient. We therefore developed a workflow in order to calculate new probe robotic parameters for standard views of patient-specific data before the procedure. Once a set of standard views of TEE are defined in the reference heart-esophagus model, the platform allows users to import any patient-specific data comprising a new heart model and esophagus centreline. These are obtained using the same automatic segmentation and manual tracing methods used for the reference heart. The method automatically calculates the specific probe robotic parameters for this patient in order to obtain the standard views defined in the reference model.

The adaption to the patient-specific heart uses iterative closest point (ICP) registration [15] to determine an affine warping of the reference heart model (along with the predefined views) to the new patient heart data. This allows more flexibility than a rigid registration while ensuring that the pre-defined view planes remain as planes after the transformation. In this process, the point sets defining the segmented surfaces of the reference and patient heart model are aligned iteratively to minimise the distance between the two point sets. For increased robustness, the heart model is divided up into separate chambers and vessels as provided by the automatic segmentation, and points in a particular section of the reference model are matched only to points in the corresponding section of the new patient model. By employing this method, a set of new standard views for the patient-specific data after registration is obtained. For each of the patient-specific standard views, the corresponding probe robotic parameters that provide this view, within the constraints of allowed probe motions, must be found. This is done by starting at the reference parameters and searching through nearby parameter values to find a new 2-D plane as near as possible to the required 2-D plane (2-D view or centre slices of 3-D view). The optimisation method employs a simple multi-resolution gradient decent search strategy in the parameter space of the kinematics. The objective function is the sum of squared distances between corresponding points within the heart on the current and required planes. Points are defined on a grid around the heart centre within the view plane. The probe position is optimised via the five robotic parameters to minimise the sum of squares of these distances. Thus, a set of robotic parameters is determined in which the required view will be obtained. The workflow of the method is shown in Fig. 3.

To study the performance of the ICP registration method and the optimisation of probe robotic parameters, 26 standard views were defined in the reference heart model. The reference was registered to two real clinical MR data. The median (IQR) error of affine registration was 11.1 (7.4-15.8) mm. The time required for the registration is within a few seconds, although this is not critical for pre-procedure planning. Correctness of the obtained views was measured as the RMS distance error between points on the obtained view plane and a manually-located gold-standard view plane. This was found to be 11.5 (8.9-15.1) mm. A qualitative assessment examined whether the obtained view plane contained all the required anatomical features of the standard TEE view, and found that 21 of the 26 views needed small adjustments while the remaining 5 needed no adjustment.

Image-based Probe Position Tracking

Once standard views for the patient-specific data are created, corresponding probe robotic parameters can be imported into the robot control system, driving the probe to perform an automatic acquisition sequence. However, considering the practical scan, manual insertion of the probe into the patient is still required for the robotic TEE approach. Therefore, knowing the initial pose of the probe head after manual insertion is essential in order to start the automatic sequence. Additionally, knowing the pose of the probe head is also important for providing feedback adjustments to improve the accuracy of the positioning. In this study, we adapted our previous work of model-based registration of pre-procedure volumetric images with trans-esophageal ultrasound images [16] to work with the view planning platform. This allows estimation of the current probe robotic parameters from the acquired 3-D ultrasound image. The images were acquired in the scanner's full-volume mode, which produces a large pyramidal 3-D image by stitching sub-volumes acquired over a few consecutive heart beats [2].

The pre-procedure MR image is segmented using the automatic method and augmented with prior knowledge of the acoustic properties of the segmented regions' tissue types. The initial estimate of the probe pose is obtained from the view planning platform, and defines a relative transformation from MR segmentation coordinates to ultrasound image coordinates. An ultrasound-like image is generated from the MR using the acoustic property information and an ultrasound imaging model. This is then registered to the real US image using a monogenic phase similarity measure [17]. The optimization method attempts to maximize this similarity measure to find the true pose of the TEE probe relative to the heart segmentation. This method has previously been shown to have a capture range of 9 mm and a median error of 2.9 mm in the registrations [16]. The registration result of the updated pose is then input to an inverse kinematic model to find the corresponding probe robotic parameters. This is achieved by searching for the probe robotic parameters in a defined range in order to best align the positions of the four corners of the transducer face on the probe head with the known probe pose. The final output of the method yields the current probe robotic parameters. The complete workflow of the method is shown in Fig. 4.

Proof of Concept: Phantom Study

Heart-esophagus Phantom and Pre-planned Views

A custom made heart-esophagus phantom (shown in Fig. 5) was built in order to provide a simulation environment for the TEE approach in terms of the movement of the probe and the image quality. A silicone tube was mounted as a representation of the esophagus. The heart phantom used was an ultrasound/MRI heart phantom (#CIRS 067, Computerized Imaging Reference Systems, Incorporated (CIRS), USA.), which is designed for viewing the heart from the anterior view. Therefore, when the phantom is placed on the box, the views of the heart are in a different anatomical orientation to those obtained in a real TEE scan. However, the proposed phantom meets most of the requirements for testing the view planning and automatic acquisition method for robotic TEE.

A special guiding mechanism was designed in order to lead the endoscopic portion of the TEE probe so that the translation movement of the robotic stage could be accurately transferred to the movement of the probe tip. The guiding mechanism includes articulation arms and a few guiding connectors. The articulation joints can be adjusted easily, forming an ideal path for the endoscopic portion of the probe. Once adjusted, the mechanism is rigidly fixed, providing a path through which the probe is advanced. In these experiments, the mechanism was set with the most distal part at 10 cm from the entrance of the phantom (or oral cavity). From there to the tip of the probe, the endoscopic portion is constrained by the silicone tube. The current design was intended for the phantom and cadaver experiments, but the same concept could be easily adapted and further improved with better features in terms of patient acceptance for clinical trials in the future. The whole experimental setup is shown in Fig. 5 with an enlarged photo of the link mechanism on the top right.

Using the custom heart-esophagus phantom, non-standard heart views were defined. A 3-D automatically segmented model of the heart was created based on an MR scan. The centre line of the tube was manually segmented. Both the segmented heart model and the tube’s centre line were loaded into the view planning platform. Based on feature structures (chambers, valves, vessels) shown in either long-axis view or short-axis view, five views were defined as follows:

- View 1 (short axis): right and left atria, pulmonary valve and aortic arch.
- View 2 (long axis): pulmonary artery, left atrium, left ventricle and pulmonary valve.
- View 3 (long axis): right atrium, right ventricle, and tricuspid valve.
- View 4 (long axis): left atrium, left ventricle, mitral valve, aortic arch, and aortic valve.
- View 5 (short axis): right and left ventricles at mid chamber.

Experimental and Post-processing Methods

The TEE ultrasound probe was inserted into the robotic system with an ultrasound machine (iE33, Philips Healthcare, The Netherlands) connected. The 3-D image data was streamed out to a PC in real time via TCP/IP. Two experiments using this setup were designed in order to test the automatic acquisition of TEE. The first experiment aimed to test the feasibility and accuracy of automatic acquisition with open-loop control. During the experiment, the probe head was manually inserted into the heart-esophagus phantom with a random starting position. A full-volume acquisition was performed and the acquired 3-D ultrasound image was registered to the MR segmentation. As described in the previous section, the image-based probe tracking method was then employed and the current probe pose was obtained. From this starting position, the robotic movement needed to obtain each target view was calculated. This step is defined as the initialization and the robot was then actuated to obtain each view relative to the known initial pose. 3-D full-volume images were acquired at each view position. This was repeated five times with different initial positions. For each of these initial positions, each view was acquired two times with the probe moving through the sequence from view 1 to view 5, then from view 5 to view 1. The second experiment aimed to test the improvement in the accuracy of the automatic acquisition using the image-based probe tracking method to provide feedback adjustments. At each iteration of adjustment, the actual position was determined by the image-based tracking and a new movement was calculated to obtain the required view. If the registration failed during the image-based tracking method, feedback adjustments were not performed and the current view was skipped. In this study, we ran the experiments and quantified the accuracy improvement over three iterations of feedback adjustments. This experiment used four different initial poses and five views for each.

For analysis of the performances of the automatic acquisition, accurate measures of the probe positions at each view were obtained using the automatic registration method described previously followed by manual corrections as needed. Errors in the probe positioning and image space were calculated by comparing the positions actually obtained to the pre-planned views. For the probe pose error, transformations from probe coordinates to the MR coordinates for planned and acquired views were calculated and decomposed to give the transformation parameters: the Cardan angles referring to rotations about the X-, Y- and Z-axes and the translation distances in the X-, Y- and Z-axes. The distance and the orientation error were defined separately as the root sum square (RSS) of the differences between the X-, Y-, and Z-axes components. For the open-loop experiment, the distance and the orientation errors of each view were calculated. For the closed-loop experiment, the distance and the orientation errors after each feedback adjustment were calculated to quantify the improvement in probe positioning accuracy after different numbers of feedback adjustments. To quantify the error in the image space, we then defined a number of marker points in the ultrasound image coordinates (90 deg * 90 deg cone, 10 cm depth). Ten image planes were selected within the TEE field of view, each parallel to the transducer of the TEE probe. The interval between two planes was 10 mm. The marker points were defined on the four corners of the image plane (Fig. 6. a). From the initial pre-planned views in the view planning platform and the acquired ultrasound views, the locations of corresponding marker points were obtained and compared in MR coordinates. As shown in Fig. 6. b, this is done by transforming the marker point locations from the ultrasound image coordinates to the MR coordinates based on the probe positions defined by the view planning platform for planned views and by the registration result for real acquired views. Mean position errors between corresponding marker points were then calculated for both open and closed loop at different depths. To analyze the influence of the initial position of the manually-inserted probe on the performance of the automatic acquisition, the mean probe pose errors of each whole sequence of five views (five sets for open-loop, four for closed-loop) were calculated. The standard deviation of these mean errors, which resulted from different initial position of the probe, was calculated to evaluate the impact of the initial probe positioning.

Performance of the Automatic Acquisition

For the open-loop method, over all the sample views, the mean position error of the probe head is 8.1 ± 2.7 mm and the mean orientation error is 11.8 ± 4.1 deg. For each of the views, the error distributions of the probe head position and orientation are summarized in Fig. 7. In the closed-loop experiment, with three iterations of the feedback adjustment, the overall mean position error of all sample views reduced from 8.5 ± 3.6 mm to 6.4 ± 2.8 mm and the overall mean orientation error reduced from 10.6 ± 4.7 deg to 8.4 ± 3.6 deg. The changes of error after each adjustment are summarized in Fig. 8.

As for the error in the ultrasound image space for open-loop and closed-loop methods, the error propagation with depth is summarized in Fig. 9, with mean errors and standard deviations for different depths. One example sequence of acquired ultrasound views using the closed-loop method is shown in Fig. 10. The ultrasound is overlaid on the MR segmentation data with long axis and short axis views shown in order to intuitively compare with the views originally defined in the view planning software.

Considering the reliability using the registration-based tracking method as feedback, of all the 20 sample views acquired in the closed-loop experiment, 3 initial registrations failed and caused failures of the feedback adjustments. Over different initial probe positions, the standard deviation in the open-loop experiment is 1.3 mm and 2.5 deg while in the closed-loop experiment it is 0.9 mm and 2.5 deg.

Discussion and Conclusion

The method of auto-adaption to patient data has been tested with real clinical data and an average error less than 1 cm was found. With small manual adjustments, the overall approach is sufficiently accurate to position the view plane close to the desired view in all cases. The source of this error is mainly the ICP registration method, in which the affine registration is not able to represent all variations in heart anatomy. Other non-rigid registration methods, such as proposed in [18, 19], may give a better alignment of the heart but the corresponding methods of identifying the standard planes and probe poses would need to be changed. As for the image-based probe tracking method, the experimental result indicates a high accuracy of the registration which is sufficient for locating the probe pose in this application. The capture range of the registration indicates a close estimation of the probe pose obtained from robotic kinematics is required in order to guarantee the success of the registration.

For the open-loop acquisition method, quantitative analysis of the error propagation in 3-D ultrasound space indicates that the error is less than 23 mm within the imaging depth of 10 cm. In a real TEE acquisition, most structures of clinical interest during cardiac procedures, including major valves and the septum, are in the near field of ultrasound (5-6 cm) where the error of the open-loop method is in the range 13.8 to 15.5 mm. With this order of magnitude of the error, it is expected that the majority of planned structures will be in the field of view and appear on the screen in 3-D mode. Therefore the open-loop method is suitable for view planning in the 3-D mode. There are a number of error sources in the method itself contributing to the overall error, including the error from initial registration, inverse kinematics, and forward modelling of the probe bending. The different errors for each view evident in Figure 7 are mainly due to the difference between the view planning software and our experimental setup. The probe is constrained to move along the esophagus centre line in the view planning software, which in reality might be different in the silicone tube. Additionally, large bi-directional bending in the silicone tube is not possible due to the rigidity of the tube. Different views defined in this study are in different portions of the silicone tube and required different ranges of bending, both of which contribute to variations of the errors. These errors will also occur in the real human body and are difficult to quantify and eliminate. Therefore, the best way to improve the accuracy is to perform acquisitions with closed-loop feedback adjustment. Considering the effect of different initial positions on the overall performance, the standard deviation results indicate that the initial position causes only small variations in the accuracy of the final probe locations. Provided the initial registration is successful, this initial position has little impact on the robustness of the solution.

Results from the second experiment using feedback adjustments indicate an obvious improvement in the accuracy of the probe positioning. Both the position and the orientation error have been reduced. From the results over multiple iterations, we can see the errors are mainly reduced in the first registration and feedback adjustment. The error of points in 3-D ultrasound space at the depth of 5-6 cm ranges from 8.0 to 9.2 mm, which is less or similar to the amount of movement and deformation of the beating heart. With the increase in accuracy, the centre slices of the obtained ultrasound image align better with the original slice view planned in Unity (shown in Fig. 10) and we believe the method with one or more feedback adjustment has great potential in providing accurate automatic acquisition not only for 3-D mode but also for 2-D mode. However, such a deviation might still cause significant challenges for the 2-D mode if a small structure is required in the view plane. In that case, a precision of few millimetres might need to be achieved, which is still challenging using the current method. The feedback method using registration has the advantage of not requiring any other sensor or equipment. However, the registration method, serving as a means of tracking, currently has limitations of computational time and reliability. The current registration method takes 10-15 seconds and has a chance of failure due to a limited capture range. Either improvement in the registration method or a failure remedy method is necessary to provide a more reliable feedback method.

Our future work aims at testing the whole view planning and the automatic acquisition method in cadavers with real TEE views to further evaluate the method in the real human body. This requires specially preserved cadavers using the Thiel embalming method [20] to allow life-like TEE acquisitions. These experiments would provide a more realistic environment in which the required level of accuracy for 3D and 2D imaging could be verified. In order to provide a faster and more reliable tracking method for feedback adjustments, electromagnetic tracking, which doesn’t rely on image quality, will be investigated for the cadaver experiments and tested together with the current image-based probe position tracking method. As a conclusion, we have presented a novel method of automatic TEE acquisition solution in this paper. The overall method not only demonstrates one important application of the TEE ultrasound robot, but also provides a new method for automatic ultrasound acquisition which can be more generally used in other types of medical ultrasound.

References

[1] J. S. Shanewise, A. T. Cheung, S. Aronson, W. J. Stewart, R. L. Weiss, J. B. Mark, *et al.*, "ASE/SCA guidelines for performing a comprehensive intraoperative multiplane transesophageal echocardiography examination: recommendations of the american society of echocardiography council for intraoperative echocardiography and the society of cardiovascular anesthesiologists task force for certification in perioperative transesophageal echocardiography," *Anesth. & Analg.*, vol. 89, pp. 870-84, 1999.

[2] A. Vegas and M. Meineri, "Core review: three-dimensional transesophageal echocardiography is a major advance for intraoperative clinical management of patients undergoing cardiac surgery: a core review," *Anesth Analg*, vol. 110, pp. 1548-73, Jun 1 2010.

[3] N. Magnavita, L. Bevilacqua, P. Mirk, A. Fileni, and N. Castellino, "Work-related musculoskeletal complaints in sonologists," *Journal of Occupational and Environmental Medicine*, vol. 41, pp. 981-988, 1999.

[4] J. A. Goldstein, S. Balter, M. Cowley, J. Hodgson, and L. W. Klein, "Occupational hazards of interventional cardiologists: prevalence of orthopedic health problems in contemporary practice," *Catheterization and cardiovascular interventions*, vol. 63, pp. 407-411, 2004.

[5] S. Wang, J. Housden, D. Singh, K. Althoefer, and K. Rhode, "Design, testing and modelling of a novel robotic system for trans-oesophageal ultrasound," *The International Journal of Medical Robotics and Computer Assisted Surgery*, 2015.

[6] P. Arbeille, J. Ruiz, P. Herve, M. Chevillot, G. Poisson, and F. Perrotin, "Fetal tele-echography using a robotic arm and a satellite link," *Ultrasound in obstetrics & gynecology*, vol. 26, pp. 221-226, 2005.

[7] S. Shah, B. A. Bellows, A. A. Adedipe, J. E. Totten, B. H. Backlund, and D. Sajed, "Perceived barriers in the use of ultrasound in developing countries," *Critical ultrasound journal*, vol. 7, pp. 1-5, 2015.

[8] L. N. LaGrone, V. Sadasivam, A. L. Kushner, and R. S. Groen, "A review of training opportunities for ultrasonography in low and middle income countries," *Tropical Medicine & International Health*, vol. 17, pp. 808-819, 2012.

[9] A. Priester, S. Natarajan, and M. Culjat, "Robotic ultrasound systems in medicine," *IEEE Trans. Ultrason., Ferroelect., Freq. Control*, vol. 60, pp. 507-523, 2013.

[10] P. Abolmaesumi, S. E. Salcudean, W. H. Zhu, M. R. Sirouspour, and S. P. DiMaio, "Image-guided control of a robot for medical ultrasound," *IEEE Trans. Robot. Automat.*, vol. 18, pp. 11-23, 2002.

[11] R. Nakadate, J. Solis, A. Takanishi, M. Sugawara, K. Niki, and E. Minagawa, "Development of the ultrasound probe holding robot WTA-1RII and an automated scanning algorithm based on ultrasound image feedback," in *ROMANSY 18 Robot Design, Dynamics and Control*. vol. 524, V. Parenti Castelli and W. Schiehlen, Eds., ed: Springer Vienna, 2010, pp. 359-366.

[12] L. Ott, F. Nageotte, P. Zanne, and M. d. Mathelin, "Robotic Assistance to Flexible Endoscopy by Physiological-Motion Tracking," *IEEE Trans. Robot.*, vol. 27, pp. 346-359, 2011.

[13] P. I. Corke, "Visual control of robot manipulators-a review," *Visual servoing*, vol. 7, pp. 1-31, 1993.

[14] J. Peters, O. Ecabert, C. Meyer, H. Schramm, R. Kneser, A. Groth, *et al.*, "Automatic whole heart segmentation in static magnetic resonance image volumes," in *Medical Image Computing and Computer-Assisted Intervention–MICCAI 2007*, ed: Springer, 2007, pp. 402-410.

[15] P. Besl and N. McKay, "A method for registration of 3-D shapes," *IEEE Trans. Pattern Anal. Mach. Intell.*, vol. 14, pp. 239-256, 1992.

[16] R. J. Housden, M. Basra, Y. Ma, A. P. King, R. Bullens, N. Child, *et al.*, "Three-Modality Registration for Guidance of Minimally Invasive Cardiac Interventions," in *Functional Imaging and Modeling of the Heart: 7th International Conference, FIMH 2013, London, UK, June 20-22, 2013. Proceedings*, S. Ourselin, D. Rueckert, and N. Smith, Eds., ed Berlin, Heidelberg: Springer Berlin Heidelberg, 2013, pp. 158-165.

[17] V. Grau, H. Becher, and J. A. Noble, "Registration of multiview real-time 3-D echocardiographic sequences," *IEEE Trans. Med. Imag*, vol. 26, pp. 1154-1165, 2007.

[18] A. Myronenko and X. Song, "Point Set Registration: Coherent Point Drift," *IEEE Trans. Pattern Anal. Mach. Intell.*, vol. 32, pp. 2262-2275, 2010.

[19] B. Fuerst, W. Wein, M. Müller, and N. Navab, "Automatic ultrasound–MRI registration for neurosurgery using the 2D and 3D LC2 Metric," *Medical Image Analysis*, vol. 18, pp. 1312-1319, 2014.

[20] S. E. Healy, B. P. Rai, C. S. Biyani, R. Eisma, R. W. Soames, and G. Nabi, "Thiel embalming method for cadaver preservation: a review of new training model for urologic skills training," *Urology*, vol. 85, pp. 499-504, Mar 2015.

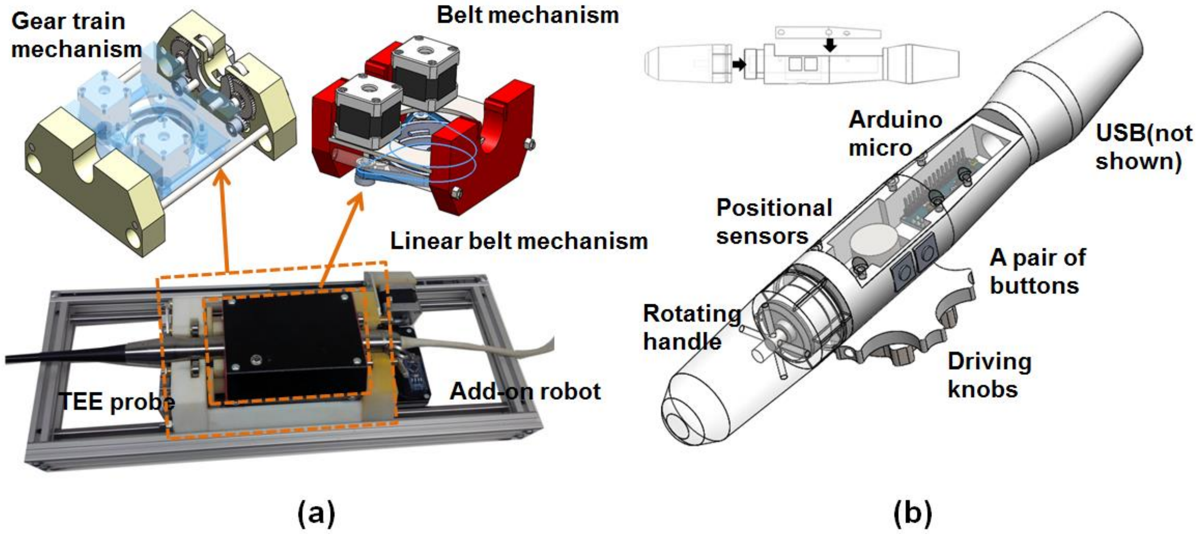

Fig. 1. Robotic system for trans-esophageal ultrasound. (a) Slave add-on driving system working together with a commercial TEE probe. (b) Master control device with positional sensors built in.

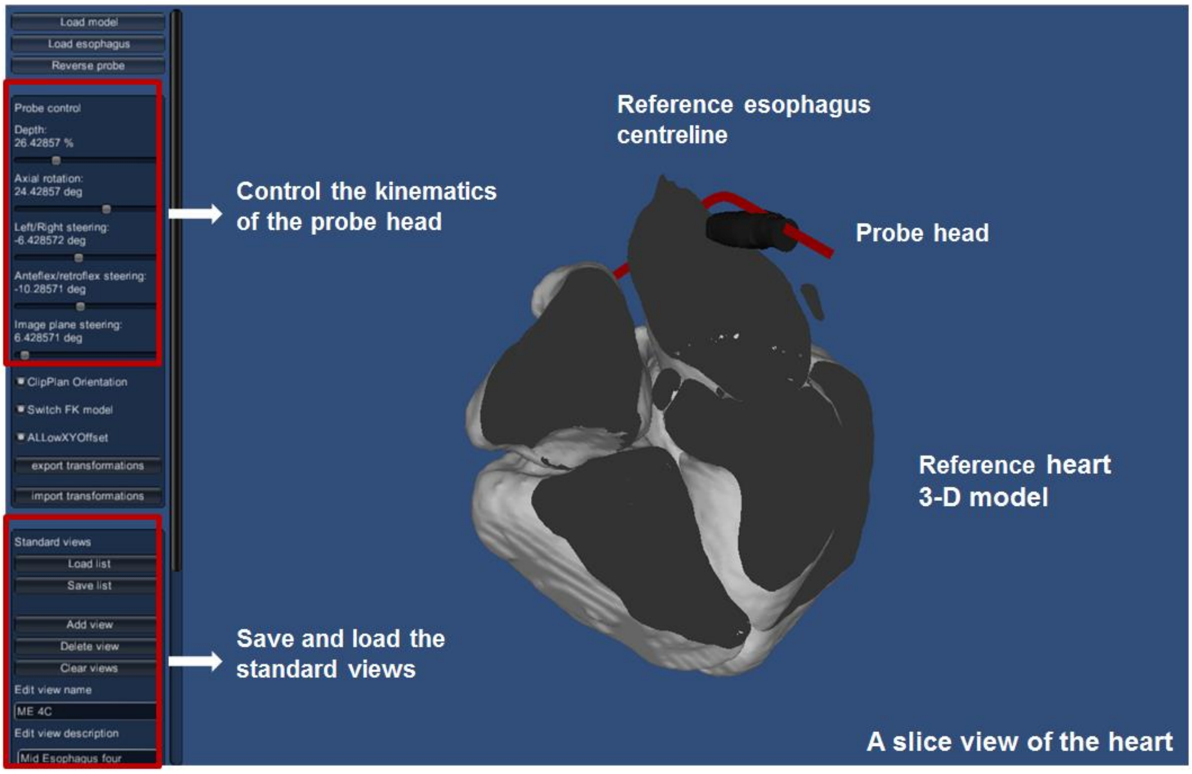

Fig. 2. Example of a 2-D mid-esophageal four chamber view shown in the view planning platform implemented in Unity. Blocks in red show the functional components of the platform.

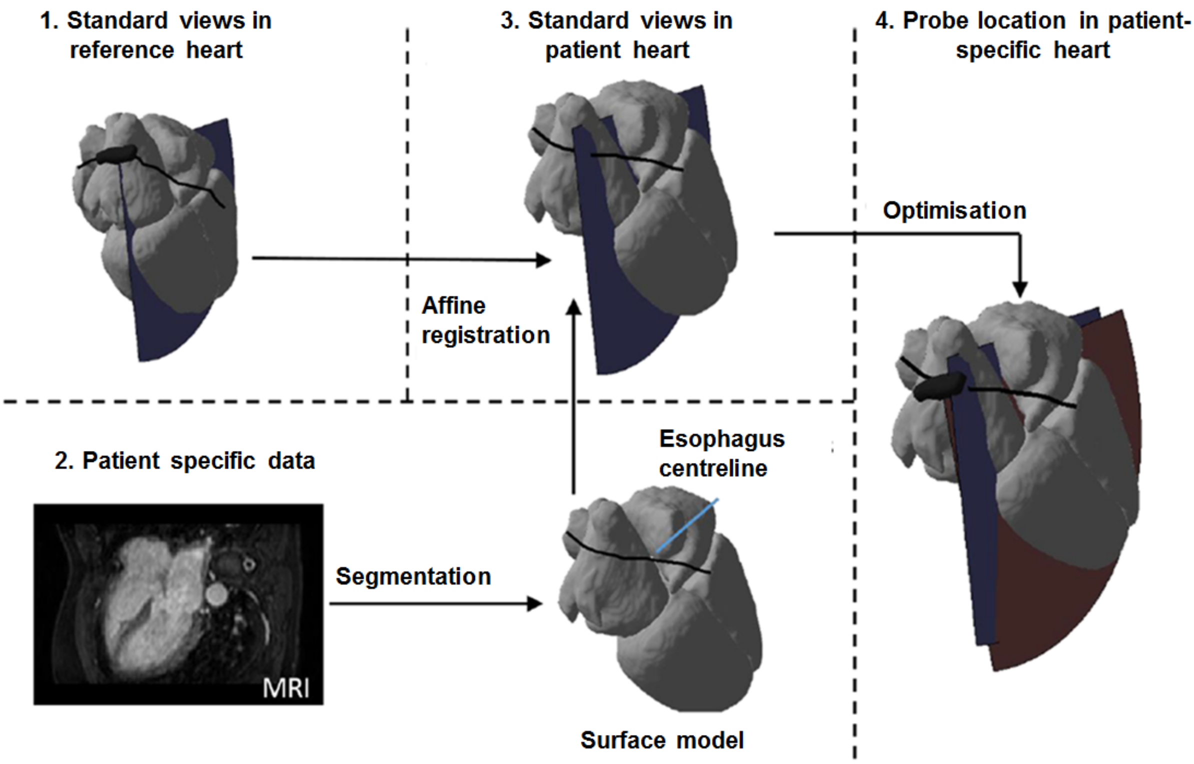

Fig. 3. Overview of the workflow to automatically calculate the probe location in patient-specific data that gives a view as close as possible to the standard view defined in the reference heart model.

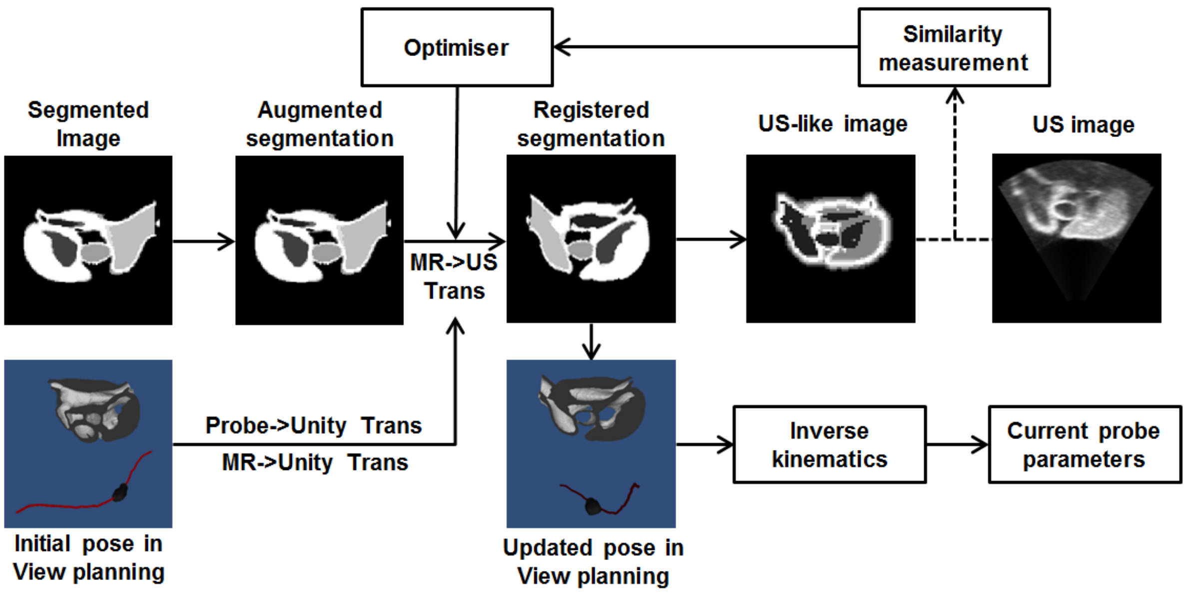

Fig. 4. Overview of the workflow to register the MR segmentation to the ultrasound image. This forms a probe position tracking method which is used to calculate the updated probe pose represented by current probe parameters.

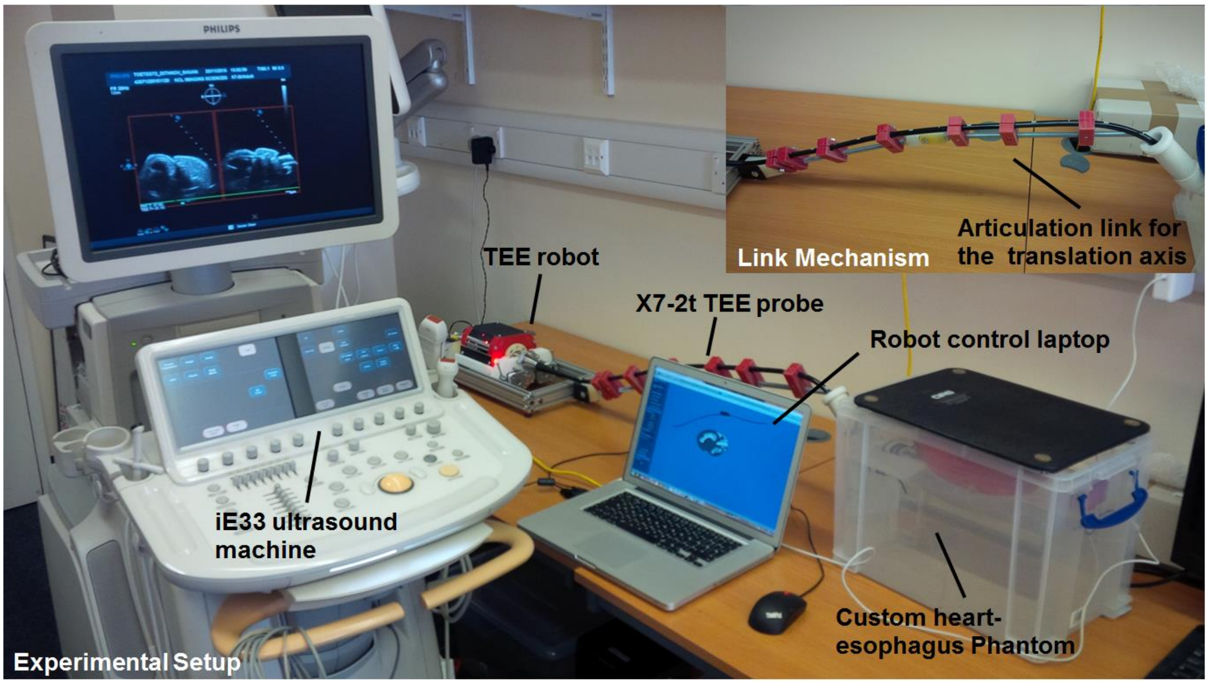

Fig. 5. Experimental setup for the phantom experiment with the TEE robot, ultrasound machine and heart-esophagus phantom. An enlarged photo of the link mechanism is shown in the top right.

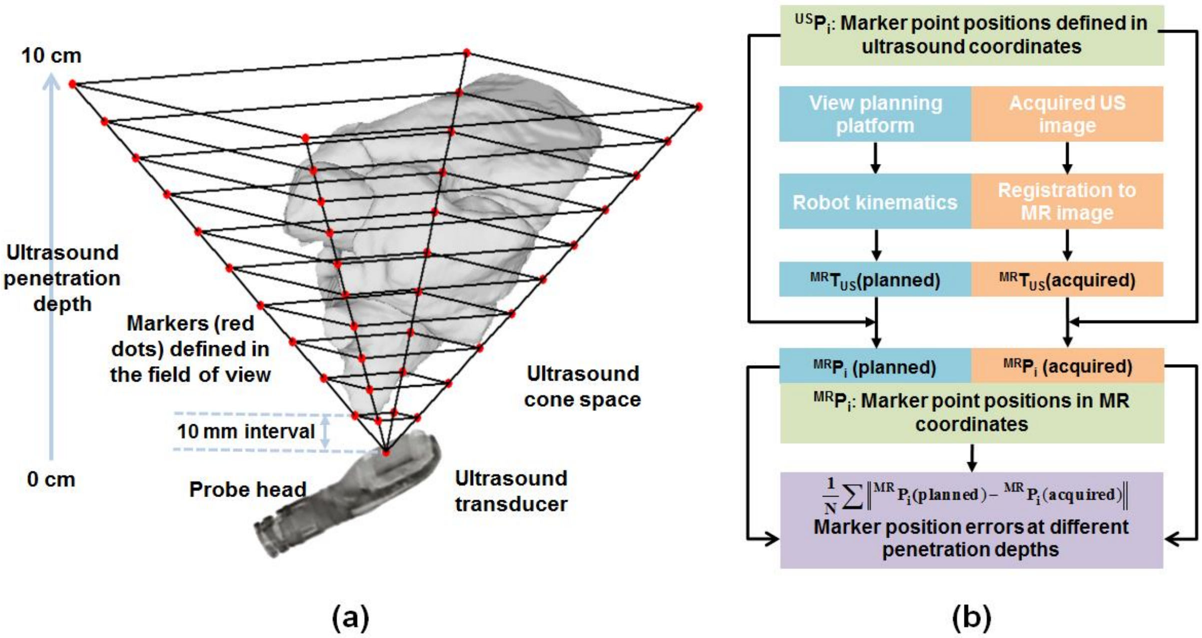

Fig. 6. (a) Marker points (red dots) defined in the ultrasound image field of view (pyramid shaped, 90 deg * 90 deg cone, 10 cm depth). Ten image planes (10 mm interval) were selected within the TEE field of view, each parallel to the transducer of the TEE probe. (b) Overview of the method using marker points defined in ultrasound coordinates to quantify the error.

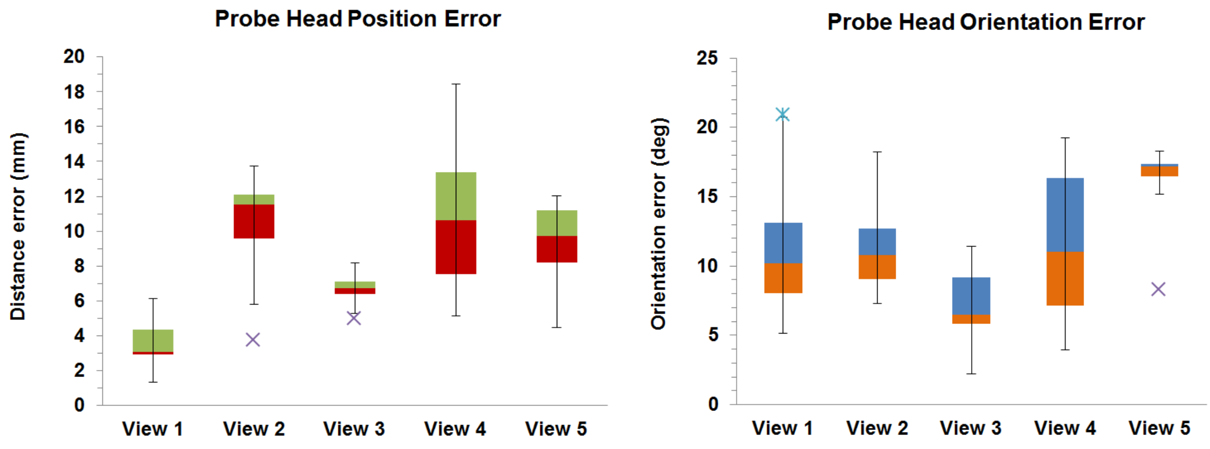

Fig. 7. Distributions of position and orientation errors (box-whisker chart) of the probe head positioning for the open-loop acquisition experiment.

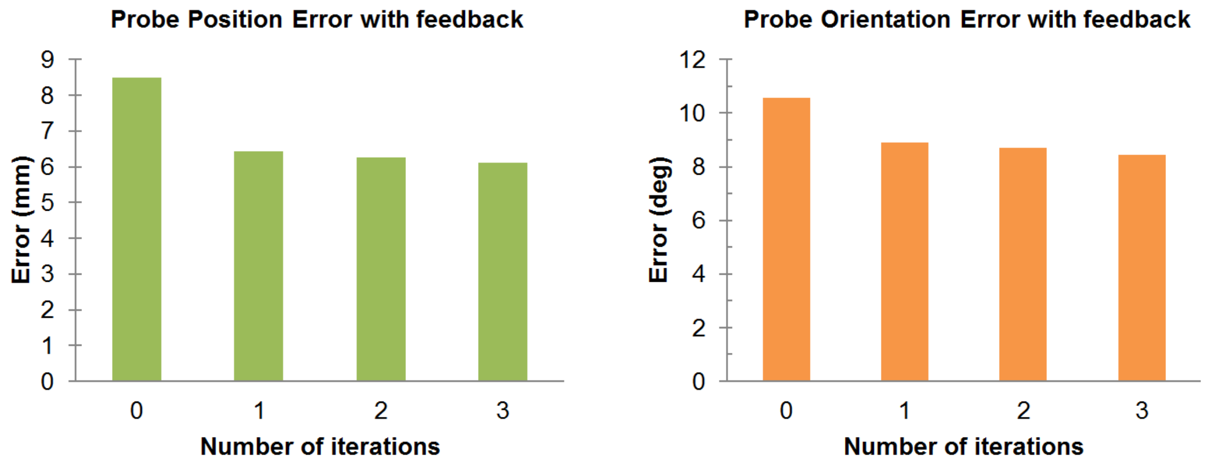

Fig. 8. Changes of the mean position and orientation errors of the probe head with different numbers of feedback adjustments employed.

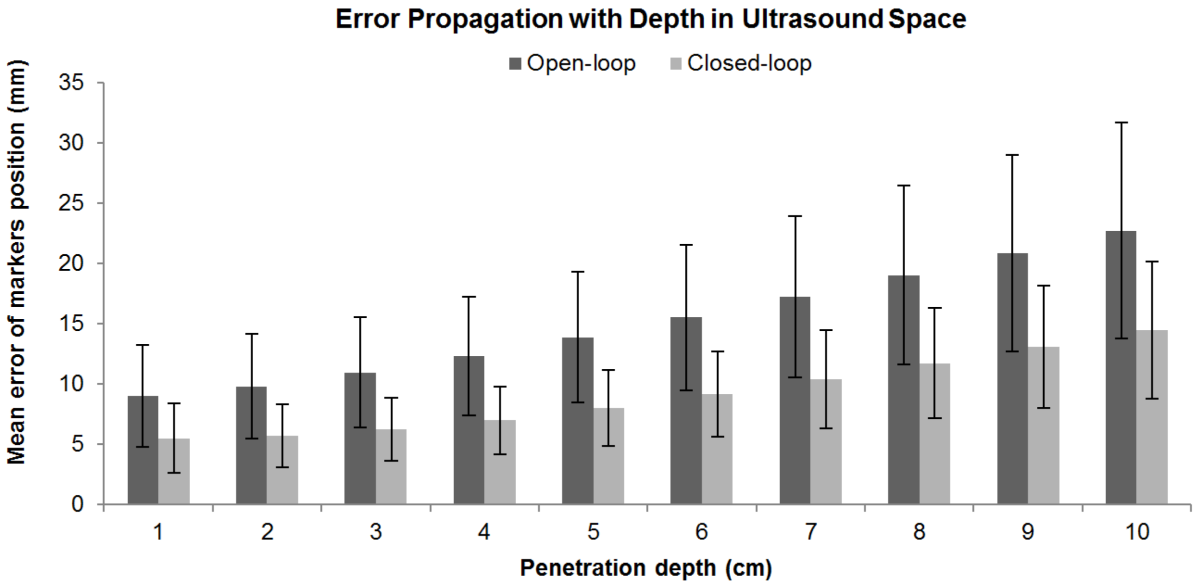

Fig. 9. Error propagation of the marker points' positions with depths in the ultrasound space for open-loop and closed-loop method.

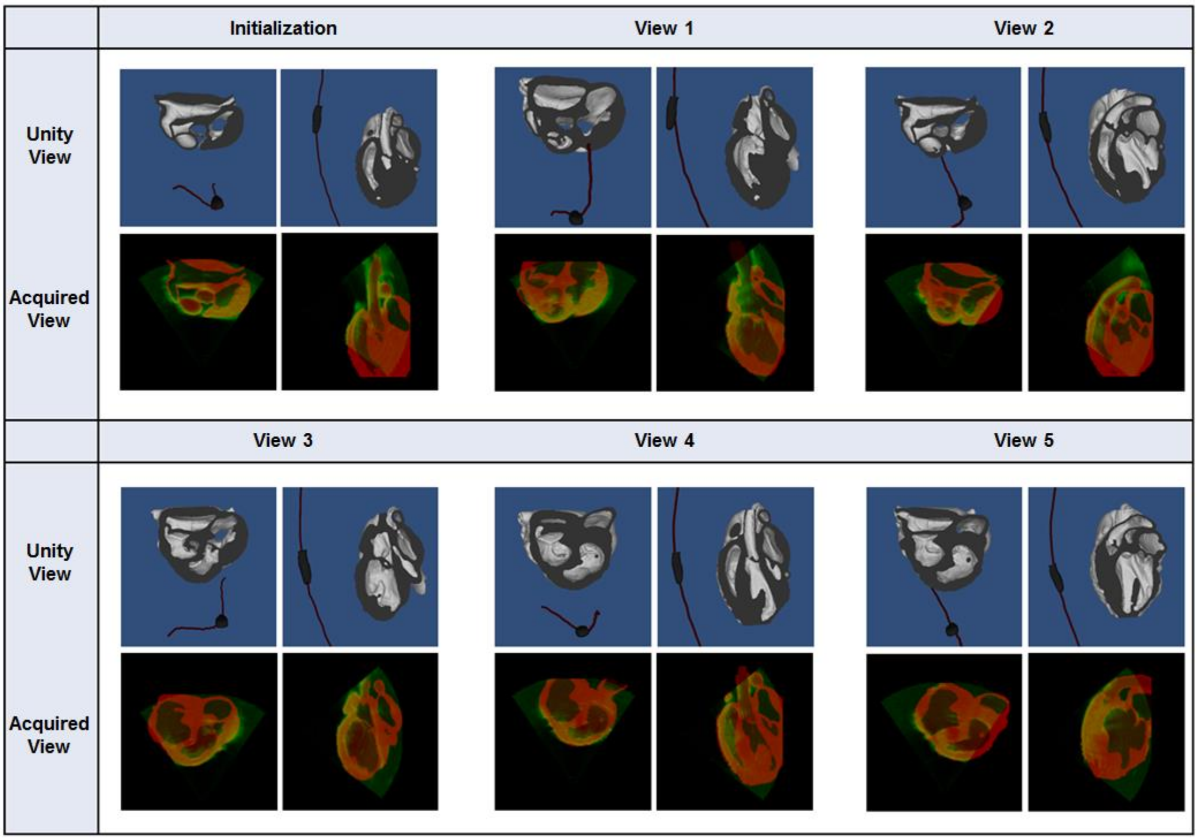

Fig. 10. Pre-planned views (long and short axis) in Unity (apart from initialization) and an example of the acquired ultrasound views (green) from the closed-loop experiment overlaid on the MR segmentation (red). For initialization, the Unity view was obtained from the acquired initial ultrasound view afterwards based on the registration and inverse kinematics.